fire

MDPI

Article

A Laboratory Study of the Effects of Wildfire Severity on Grain Size Distribution and Erosion in Burned Soils

Deepa Sapkota, Jeevan Rawal, Krishna Pudasaini and Liangbo Hu *

Department of Civil and Environmental Engineering, University of Toledo, Toledo, OH 43606, USA; deepa.sapkota@rockets.utoledo.edu (D.S.); jeevan.rawal@rockets.utoledo.edu (J.R.); krishna.pudasaini@rockets.utoledo.edu (K.P.)
* Correspondence: liangbo.hu@utoledo.edu

Abstract: Wildfires pose a significant threat to the entire ecosystem. The impacts of these wildfires can potentially disrupt biodiversity and ecological stability on a large scale. Wildfires may alter the physical and chemical properties of burned soil, such as particle size, loss of organic matter and infiltration capacity. These alterations can lead to increased vulnerability to geohazards such as landslides, mudflows and debris flows, where soil erosion and sediment transport play a crucial role. The present study investigates the impact of wildfire on soil erosion by conducting a series of laboratory experiments. The soil samples were burned using two different methods: using firewood for different burning durations and using a muffle furnace at an accurately controlled temperature within 400 °C∼1000 °C. The burned soils were subsequently subjected to surface erosion by utilizing the constant head method to create a steady water flow to induce the erosion. In addition, empirically based theoretical models are explored to further assess the experimental results. The experimental results reveal a loss of organic matter in the burned soils that ranged from approximately 2% to 10% as the burning temperature rose from 400 °C to 1000 °C. The pattern of the grain size distribution shifted to a finer texture in the burned soil. There was also a considerable increase in soil erosion in burned soils, especially at a higher burn severity, where the erosion rate increased by more than five times. The empirical predictions are overall consistent with the experimental results and offer reasonable calibration of relevant soil erosion parameters. These findings demonstrate the importance of post-fire erosion in understanding and mitigating the long-term effects of wildfires on geo-environmental systems.

Keywords: wildfire; soil; debris flow; entrainment; erodibility

Academic Editor: Raffaella Lovreglio

Received: 22 December 2024
Revised: 20 January 2025
Accepted: 22 January 2025
Published: 25 January 2025

Citation: Sapkota, D.; Rawal, J.; Pudasaini, K.; Hu, L. A Laboratory Study of the Effects of Wildfire Severity on Grain Size Distribution and Erosion in Burned Soils. *Fire* **2025**, *8*, 46. https://doi.org/10.3390/fire8020046

1. Introduction

Wildfires have become a recurring natural threat in the United States, often exacerbated by climate change, land use patterns and anthropological activities. The western part of the country is especially prone to wildfires due to its arid climate and abundant forests and grasslands. Every year, it often experiences a large number of wildfires that have been increasing in both size and frequency in recent decades. Wildfires can have long-term impacts on soil behavior, including the physical, chemical and biological properties, as well as far-reaching effects on the microbial communities and geological processes [1–3]. Post-wildfire impacts on the environment are multifaceted and can have significant ecological and economical implications, such as water quality deterioration [4–6], land loss [7,8] and livestock health and production [9]. For geotechnical engineering communities, of particular interest is the prospect of post-wildfire soils becoming more vulnerable to various

geological hazards, such as landslides, mudslides, debris flows and flash floods. Indeed, such incidents of landslides and debris flows, which are often triggered by intensive rainfall, have been widely reported following the fire seasons in the western US [10–12]. Post-wildfire soils are affected by two key phenomena that are possibly responsible for their compromised stability. First, the soils appear more resistant to water infiltration, thus leading to increased overland flow or surface runoff [13,14]. Secondly, they may become more susceptible to erosion and thus they have much greater potential to generate massive flows of debris material [15–17]. Hence, post-wildfire runoff and erosion are major concerns in fire-prone landscapes globally [18].

Research studies by Rengers et al. [19] and Orem and Pelletier [20] have shown that wildfires can cause a significant increase in erosion due to changes in soil erodibility and water infiltration, persisting for several years following the wildfire event. Elliot and Flanagan [21] demonstrate that the erosion following a wildfire can be many times the erosion from an undisturbed forest, based on the investigation of 36 soil sites from nearly 20 states of the United States. Post-fire soil erosion is of considerable concern due to its potential adverse effects on downstream resources and site productivity [22]. Turnbull et al. [23] explored the impact of fire severity on soil erosion in shrublands, highlighting the role of vegetation loss and hydrophobic soil surfaces in increased erosion rates. Raindrop-driven erosion processes have been identified as particularly important in the incipient stages of rill formation in post wildfire settings [24]. The hydrologic response to wildfires in mountainous regions can increase higher runoff and erosion, posing risks to life and infrastructure [25].

Post-wildfire floods with severe erosion have been observed in various regions, demonstrating the importance of accurate predictions of the magnitude of post-wildfire flow and erosion potential [12,26]. The effects of wildfires on soil properties vary with fire intensity, severity, frequency and size, leading to changes in soil erodibility and hydraulic properties [14,27,28]. In addition to many case studies in the United States, field investigations around the world have also reported considerable evidence in the change in sediment erosion after wildfires. In a case study of fire-induced erodibility at La Costera, Valencia, southeast Spain, the sediment yield, sediment concentration and erosion rates were found to be 35.26, 12.45 and 37.845 times higher, respectively, two years after the fire than ten years after the fire by Cerda et al. [29]. Follmi et al. [30] investigated the large wildfires in the Mediterranean ecosystems that impacted sediment redistribution over multiple decades, leading to increased erosion and deposition rates. Yang et al. [31] studied the 2019–2020 wildfires and storm events in the Sydney Drinking Water Catchment and identified a significant increase in erosion rates.

The rise in widespread and intense wildfires presents significant environmental challenges, as the wildfires leave the landscape vulnerable to erosion and pose potential far-reaching threats to ecosystems, water quality and human communities. Understanding post-wildfire erosion dynamics is crucial for developing effective mitigation strategies and sustainable land management practices. The severity of erosion is influenced by a range of factors, such as rainfall intensity, soil properties and burn severity [32,33]. Soil texture and organic matter content are critical factors in erosion susceptibility [34]. Hence, it is of benefit to carry out a laboratory-scale experimental investigation to focus on the fundamental characteristics of burned soils and assess their change in erodibility. The primary objective of the present study is to explore the evolution of basic geotechnical characteristics before and after the burning, with a specific focus on the soil erosion. In the present study, a series of experiments are explored using two methods of soil burning for specific durations or at controlled temperatures to simulate the effects of different burn severities. The pre- and post-fire properties of a typical surficial soil are examined, including the change in

organic matter, particle size distribution and plasticity. The surface erosion of tested soil samples is also investigated, and relevant theoretical erosion models are explored to assess the experimental results and evaluate the key erosion parameters.

2. Experimental Investigation

2.1. Materials and Burning Methods

In the present study, soil samples were collected from the streambank of the Ottawa River located in the campus of the University of Toledo, Toledo, Ohio, USA. Two burning methods were explored to simulate the effects of the wildfires on soil behavior. The first burning method was conducted outdoors using firewood (hereafter referred to as fire burning) (Figure 1). Wood was placed and ignited on the soil in a 60 cm × 60 cm tray of 13 cm depth, with additional wood added continuously to maintain the fire for the specified duration. To simulate varied fire severities, after a number of trials, soil samples were subjected to burning for three durations: one hour, two and a half hours and four hours, aiming to represent a low, moderate and high severity of burning. The temperature on the soil surface was measured using an infrared thermometer laser temperature gun, which found that the highest temperature reached was approximately 720 °C.

Figure 1. Fire burning of soil samples with wood.

Figure 2 shows the burned soil samples of varied severity: the low severity burning shows the presence of black ash on the soil, while the visual indicator of moderate severity is gray ash and the visual indicator of high severity is white or orange ash. This is consistent with the description of burning severity suggested by Wells et al. [35] and DeBano et al. [7].

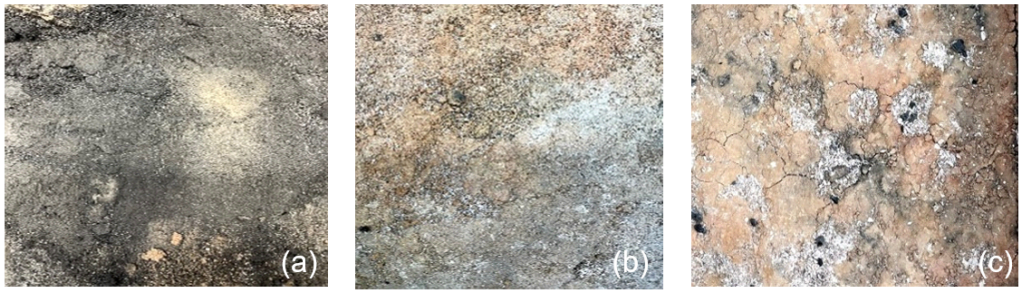

Figure 2. Photos of soil samples after (**a**) low-severity burn; (**b**) moderate-severity burn; (**c**) high-severity burn.

The second method was explored using a muffle furnace with the principal aim to precisely control the temperature. This muffle furnace (Model MF-2A, Gilson Inc.,

Lewis Center, OH, USA) can reach the highest temperature of 1287 °C. Another primary motivation of exploring this method is that outdoor fire burning is often restricted by local fire regulations, while oven heating is free of such restrictions and weather constraints. Soil samples were heated in the muffle furnace for one hour at a controlled temperature of 400 °C, 600 °C, 800 °C or 1000 °C. A muffle furnace typically requires sophisticated procedures for temperature control due to the exceptionally high temperature involved. During this heating, in the present study, the targeted temperature was raised in half an hour, then maintained at that temperature for one hour and finally dropped to room temperature in half an hour. The selection of the temperature range in the present study is consistent with the typical temperatures at the soil surface during the wildfires reported in the past research findings [36–38]. It represents the wide temperature range during wildfires, allowing one to assess soil responses to different thermal conditions and simulate the varied burning severity. For the sake of convenience, this method is hereafter referred to as oven burning (in contrast to fire burning). Figure 3 shows the visual observations of color changes in the soil samples, where more soil particles turned to orangish at higher temperature. In this oven burning test, it becomes also possible to assess the loss of organic matter during the burning. Soil organic matter helps to bind soil particles, forming aggregates that improve drainage and aeration, thus preventing erosion and compaction.

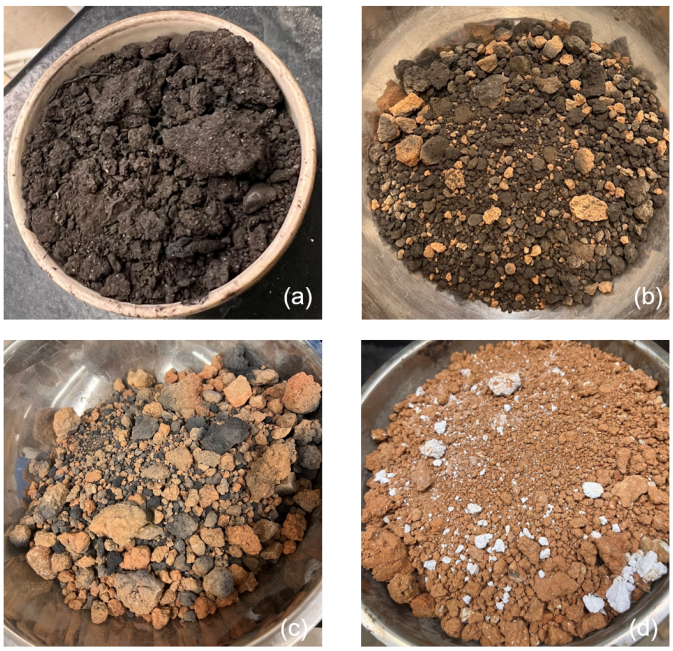

Figure 3. Photos of soil samples after burning in the furnace at the temperature of (**a**) 400 °C; (**b**) 600 °C; (**c**) 800 °C; (**d**) 1000 °C.

2.2. Fundamental Characteristics

The grain size distribution of soil samples generally plays an important role in their behavior. Especially during the wildfires, the burning may lead to considerable changes in the particle sizes [39–41] that impact the post-wildfire soil behavior. In the present study, sieve analysis and a hydrometer test were carried out to identify the grain size distribution of the original samples as well as the burned samples.

Figure 4 shows the grain or particle size distribution (PSD) of all four soil samples examined in the fire burning, including the original and three burned samples. There is some modest alteration in the soil texture. Overall, the distribution curve tends to shift toward the left, i.e., certain fractions of grains became smaller. However, a close examination is necessary to identify the subtle details of such evolution.

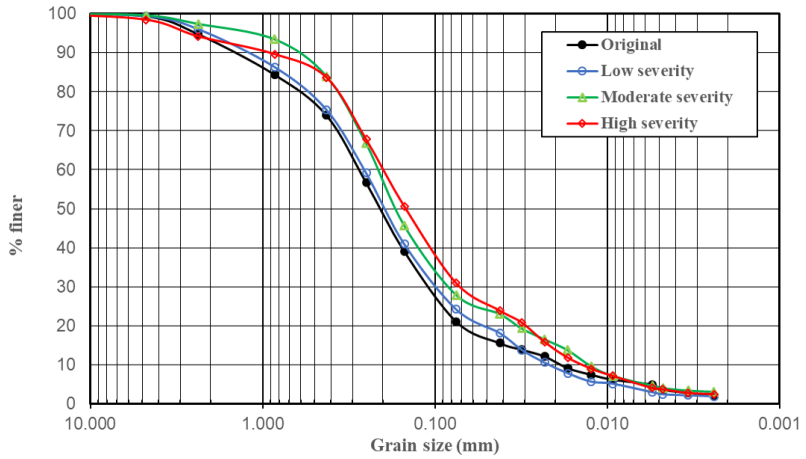

Figure 4. Grain size distribution of four soil samples examined in the fire burning.

The original soil sample consisted of 0.6% gravel (particles larger than 4.75 mm), 78.4% sand (particles between 4.75 mm and 0.075 mm), 19.1% silt (particles between 0.075 mm and 0.002 mm) and 1.9% clay (particles smaller than 0.002 mm). In geotechnical engineering, the combination of the silt and the clay together is typically referred to as the fines. The low-severity burning resulted in a shift toward finer soil textures, with a considerable increase in silt to 22.3%, while the sand fraction decreased to 75.3% and the clay fraction almost remained the same. This pattern is consistent as the burning severity changed from low to moderate and then to high, culminating in a final composition of 67.6% sand, 28.5% silt and 2.4% clay for the high-severity burned samples. Notably, the clay content experienced a subtle decrease in the high-severity sample compared with the moderately burned sample, in contrast to the general trend of increasing fines. These results reveal an interesting trend: as the severity of the fire increased, there was a slight increase in the fine fractions of the soil, i.e., silt and clay. Meanwhile, this increase was accompanied by a corresponding decrease in the sand fraction. It is worth noting that, with increasing fire severity, there was a marked decrease in sand particle percentage. This may be indicative of thermal decomposition and subsequent fragmentation or disintegration of coarse particles into smaller material.

Similarly, the particle size distribution of soil samples burned at different oven temperatures was also experimentally determined, as shown in Figure 5. It is observed that a similar general trend to the fire burning emerged. When comparing the original unburned sample with the burned samples, the finer soil fractions, i.e., specifically the silt and the clay, experienced a slight increase, while the sand fraction exhibited a slight decrease.

In the sample subjected to a low-temperature burn at 400 °C, there is an overall shift toward a finer texture. The silt and clay percentages rose from 19.1% and 1.9% to 21.1% and 4.3%, respectively, while the sand content decreased from 78.4% to 73.1%. This trend continued and was more pronounced at 600 °C, with the sand further decreasing to 74.3% and the silt increasing to 22.5%, in despite of the clay dropping to 1.1%. However, the samples burned at higher temperatures of 800 °C and 1000 °C seemed to experience a certain rebound toward the original PSD: the fines content decreased while the sand fraction increased from those at lower temperatures. For example, in the sample after 1000 °C burning, the fine particles and sand particles were 22.3% and 77.9%, respectively, which are not very different from those of the original soil sample.

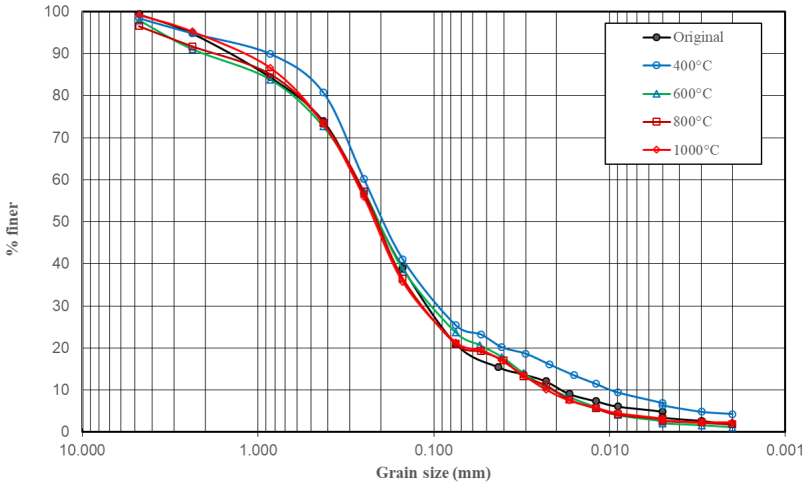

Figure 5. Grain size distribution of all soil samples examined in the oven burning.

A plausible explanation could be attributed to the possibility of grain agglomeration at higher temperatures, where the fine particles that are disintegrated begin to accumulate or clump together. This process compensates for the initial increase in fine particles due to the breakdown of larger particles. The observation aligns with the hypothesis that soil undergoes both breakdown and agglomeration processes under the influence of heat, with the dominance of either process dependent on the severity of the burning.

The Atterberg's limits test for soil consistency is a crucial geotechnical test for determining the critical water content at which fine-grained soils transition between different states: rigid, plastic and liquid. The behavior of soils is significantly influenced by their water content. This is particularly relevant for soils containing a notable amount of fines, which exhibit varied engineering behavior based on the in situ moisture levels. The primary focus of this test in the present study is to identify the changes in the physical properties of soil, especially plasticity and consistency, following the exposure to different burning conditions. These properties are fundamental in defining soil behavior and are relevant to various aspects, such as post-fire stability, compressibility and the soil's interaction with drying/wetting cycles.

In the present study, the liquid limit (LL) and the plastic limit (PL) tests were carried out on both original and burned samples. Table 1 summarizes the results for the original soil sample. The plastic index (PI) represents the range of water content over which the soil behaves plastically. Combining these results with the particle size distribution (PSD) analysis, the soil is classified as clayey sand. This classification is based on the soil's granular composition and its behavior within the plasticity chart, which aligns with the criteria for clayey sand in accordance with the Unified Soil Classification System (USCS).

Table 1. Summary of Atterberg's limits of the original soil.

Parameter	Value
Liquid Limit	38
Plastic Limit	24
Plastic Index	14

Interestingly the Atterberg's limits test on each of the burned samples, either from fire or oven burning, turned out not to be possible due to the altered texture after the burning. The burned soil resembled crushed stone dust with minimal cohesion and exhibited no plasticity at all. This distinctive lack of plasticity may be attributed to the transformation of clay minerals upon exposure to high temperatures. Typically, soil plasticity is

primarily influenced by its clay content. When subjected to heat during the burning, the hydroxyl groups within the clay's crystalline structure might tend to expel each other. This alteration changes the properties of the soil, resulting in the observed loss of plasticity. Consequently, it became impractical to determine the liquid limit and plastic limit values for the burned soil, since it was not able to form a cohesive paste when mixed with water to sustain the blowing or rolling specified in the procedure. It was evident that the burned soil no longer demonstrated the cohesive properties required due to the alteration in its mineral composition.

In addition, in the oven burning, it is possible to assess the loss of the organic matter in the soil sample by measuring the total mass of the sample before and after burning. It is noted that, initially, the original soil sample was subjected to conventional oven drying at the temperature of 105 °C for 24 h to remove all its moisture content, before being transferred to the muffle furnace at the controlled temperature ranging from 400 °C to 1000 °C.

It is assumed that the difference between the initial and final masses of the sample provided the measure of organic matter loss because such high temperatures are generally believed to be able to break down the organic matter [42,43]. Figure 6 shows the percentages of mass loss at different burning temperatures. As the temperature rose, the loss of organic matter also increased and appeared almost in a proportional relation with the temperature in the tested temperature range. This seems to suggest that a higher temperature induces greater decomposition of organic matter. However, it is worth noting that there might be other factors or processes in play, especially at a very high temperature. Potential other chemical reactions in the presence of oxygen in a confined space of the furnace may result in a variety of reactants and products, affecting the overall mass. More comprehensive fundamental research may be needed in further studies to identify the key processes.

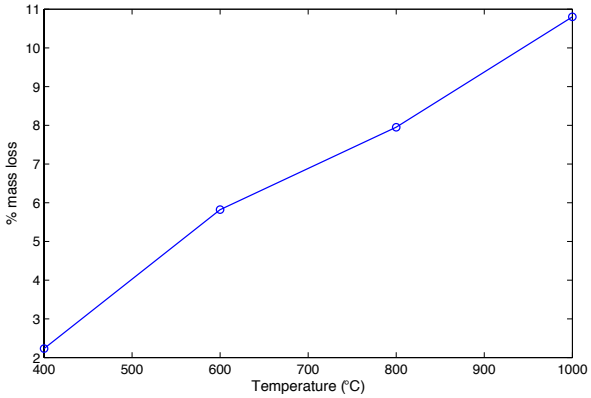

Figure 6. Percentage of mass loss in oven-burned samples.

2.3. Surface Erosion

Each soil sample was gradually transferred to a 22 cm (length) × 11 cm (width) × 6.3 cm (depth) tray inclined at a 25° angle (Figure 7). It was transferred to the tray in three layers, each of which was compacted before the next layer was placed. After the excess soil was removed from the smoothened surface, the soil was subsequently subjected to a steady water flow driven by a constant head difference setup for two minutes. The eroded mass was then collected and oven-dried, and the measured eroded mass was used to quantify surface runoff under different simulated wildfire scenarios.

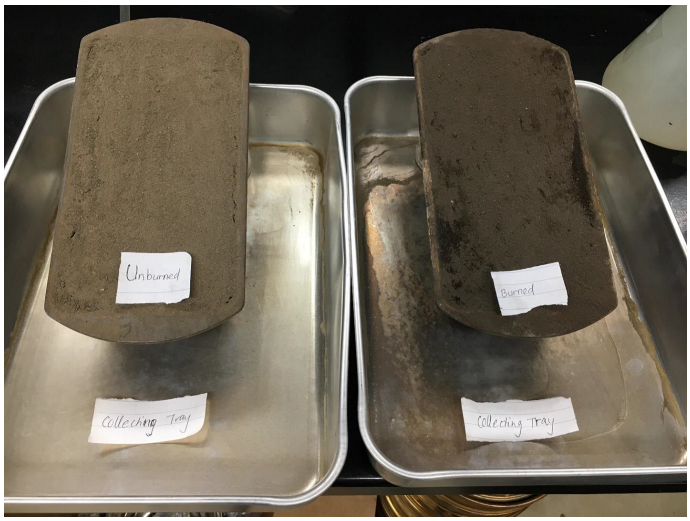

Figure 7. Original (unburned) and burned soil samples subjected to surface erosion. Note that the sample corresponding to a (room) temperature of 20 °C indicates the original unburned soil, the temperature of 400 °C indicates low-severity burn, 600 °C indicates moderate-severity burn and 800 °C and 1000 °C indicate high-severity burn.

Figure 8 presents the results of the eroded soil mass over the sample surface in the original and fire-burned soil samples. For the soil at each burn severity, three samples were tested, with the averaged values being reported. As discussed in Section 2.1, the durations of 1, 2.5 and 4 h correspond to low-, moderate- and high-severity burning, respectively. It shows that soil erosion was significantly higher in burned soil samples compared to unburned soil samples. The erosion in the severely burned sample increased by more than five times compared with the original soil sample. The rise in burning severity seems to considerably enhance the susceptibility of erosion, as the high severity led to more than double the erosion under low severity.

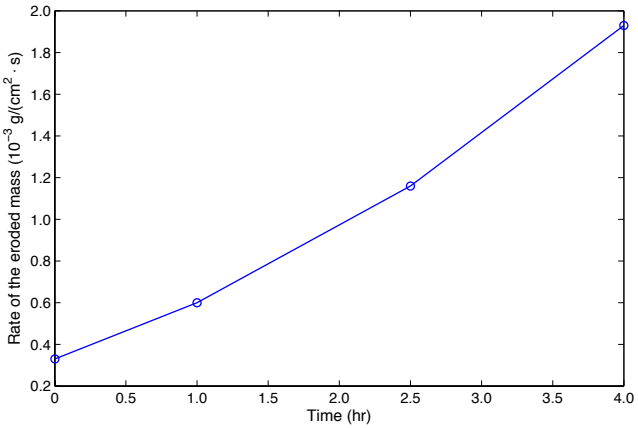

Figure 8. Eroded soil in the original and fire-burned soil samples. Note that the sample after a burning time of 0 indicates the original unburned soil, the duration of 1 h indicates low-severity burn, 2 h indicates moderate-severity burn and 4 h indicates high-severity burn.

Similar tests were also conducted in the oven-burned samples. It is worth noting that, due to the limited oven capacity, which only allowed roughly 250 mL of soil burning inside, it took six or seven burnings to accumulate needed soil for each erosion test. Only one such accumulated soil assembly was tested for the surface erosion. Figure 9 shows the eroded soil mass in the original and oven-burned soil samples. Evidently, there was a significant increase in the erosion at higher temperatures, although the further change beyond 600 °C

was not very substantial. Overall, the eroded masses were reasonably comparable with those in the fire-burned samples, which were somewhat higher under the high severity.

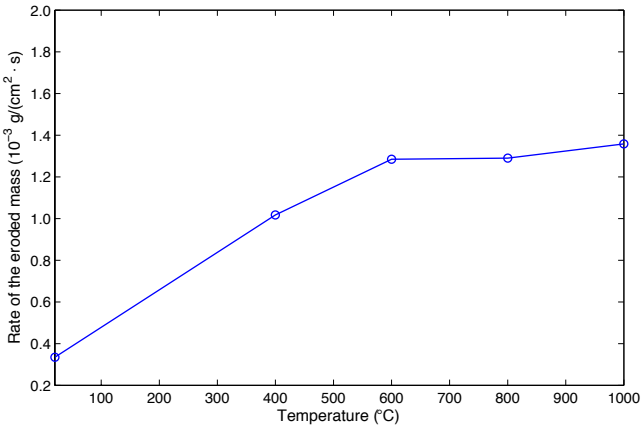

Figure 9. Eroded soil in the original and oven-burned soil samples. Note that the sample corresponding to a (room) temperature of 20 °C indicates the original unburned soil, the temperature of 400 °C indicates low-severity burn, 600 °C indicates moderate-severity burn and 800 °C and 1000 °C indicate high-severity burn.

3. Assessments of Key Parameters for Erosion Models

It is of great interest to explore the surface erosion from a theoretical perspective based on commonly used numerical models in practice. There are a wealth of empirical models developed, such as the Universal Soil Loss Equation (USLE), Revised Universal Soil Loss Equation (RUSLE) and other associated models (e.g., RUSLE2), for the estimation of erosion rates. The USLE model estimates the average rate of soil erosion based on the crop system, soil types, rainfall pattern, topography and land cover [44]. The RUSLE is a revised form of the USLE and offers several improvements to estimate the factors in the USLE [45–47]. Another derivative of these types of models, RUSLE2, offers a computer interface that can handle complex field conditions [48]. These models were initially developed focusing on applications in the United States; however, they are now applied globally for long-term land management to assess the sediment yield or soil loss [49–53]. Other empirical and numerical models include the Kinematic Runoff and Erosion Model (KINEROS) [54], the Watershed Erosion Prediction Project (WEPP) [55], the Kinematic Runoff and Erosion Model-2 (KINEROS-2) [56], the Soil and Water Assessment Tool (SWAT) [57], etc. Some of the models are implemented in GIS-based simulation tools that are capable of simulating overland flow and erosion over an actual topography, such as the Automated Geospatial Watershed Assessment (AGWA) tool, which is one of the most popular modeling software of its type [58–60].

In various families of erosion models, one of the most crucial parameters used for the estimation of eroded sediment is the erodibility factor. This factor is defined as the soil loss per unit of rainfall erodibility index, and it is determined by the amount of soil loss caused by various erosive forces, such as rainfall, runoff or seepage, within a standardized unit [61,62]. It is influenced by factors including soil physical properties, vegetation cover and land use types [63]. Several empirical equations have been developed for estimating this parameter based on the physical properties of soil, particularly the grain size distribution [44,45,49,64–66]. The model proposed by Wischeimer and Smith [44] is widely used in the USA; it has been adopted by the Natural Resources Conservation Service (NRCS) to develop the Soil Survey Geographic (SSURGO) database. Based on the experimental results of particle size distribution reported in Section 2, it is therefore possible to further explore the empirical estimation of the erodibility and the relevant erosion rate.

In the present study, the erosion model based on the work of Engelund and Hansen [67] for sediment transport, which was later implemented in the AGWA simulation tool, is adopted to assess the post-fire erosion rate and the erodibility, as calibrated from the experimental results. It is considered as suitable for the overland flow erosion estimation in upland areas in terms of accuracy [68]. Of relevance to the present study is the hydraulic erosion rate, e_h, proposed as linearly dependent on the difference between sediment transport capacity (C_m) and sediment concentration (C_s) [69]:

$$e_h = c_g(C_m - C_s)A \tag{1}$$

where A is the flow area, and the key parameter, c_g, is the transfer rate coefficient, which is calculated based on land cover and soil type. Smith et al. [54] proposed the following empirical relationship for clay content of no more than 22%:

$$c_g = \frac{5.6K\phi_r}{188 - 468\alpha_{cl} + 907\alpha_{cl}^2} \tag{2}$$

where ϕ_r is the erosion resistance factor due to mulches or the duff layer and K is the aforementioned soil erodibility factor and is detailed further subsequently. α_{cl} is the fraction of clay. For clay content of more than 22%, a different empirical estimation was suggested:

$$c_g = \frac{5.6K\phi_r}{130} \tag{3}$$

The sediment capacity, C_m, represents the concentration at equilibrium transport capacity, while C_s is the concentration at any considered time, which is typically zero initially and increases as the concentration in the flow increases. Based on Engelund and Hansen [67], the sediment capacity can be estimated via the following:

$$C_m = \frac{0.005uu_*^3}{g^2dh(G_s - 1)^2} \tag{4}$$

where u is the velocity of flow, u_* is the shear velocity, d is the particle diameter, h is the flow depth and G_s is the specific gravity of soil particles.

To estimate the key parameter of the soil erodibility factor, K, various empirical formulas and methods have been developed based on soil survey data and field measurements. There were a number of models proposed for soil erodibility [64–66] that solely focus on soil particle size, specifically sand, silt and clay. The present study adopts the approach employed by the AGWA model, which uses the R/USLE equation for soil erodibility as in the following:

$$K = \frac{2.1M^{1.14}(10^{-4})(12 - a) + 3.25(b - 2) + 2.5(c - 3)}{100} \tag{5}$$

where M is an intermediate parameter involving the fractions of silt, fine sand and clay.

$$M = (\alpha_s + \alpha_{fs})(100 - \alpha_{cl}) \tag{6}$$

α_s is the percentage of silt, α_{fs} is the percentage of fine sand (0.075 mm $\sim$ 0.425 mm) and α_{cl} is the percentage of clay. a is the percentage of organic matter, while b is an index value (1$\sim$4) used for soil classification: 1 for fine granular soil, 2 for fine granular, 3 for medium or coarse granular and 4 for platy or blocky soil. The parameter c is an index (1$\sim$6) accounting for soil permeability, ranging from rapid (1) to very slow (6).

Based on these empirical estimations, which can utilize the particle size distribution data discussed in Section 2, Equations (5) and (6) are used to calculate the erodibility factor for the original and burned soil samples. Figures 10 and 11 present the value of the erodibility factor for fire-burned and oven-burned soil samples, respectively. The evolution of the erodibility factor in fire-burned samples seems to consistently increase with the duration and severity of the burning, since the pattern of grain size distribution in these samples is very consistent as the fine sand fraction as well as the silt fraction increases, while, in the oven-burned samples, as discussed in Section 2.2, such a trend is reversed in the samples under the high temperature (e.g., 800 °C and 1000 °C) when the fine sand fraction as well as the silt fraction begins to decrease slightly; hence, the estimated erodibility factor somewhat decreases at the high temperature.

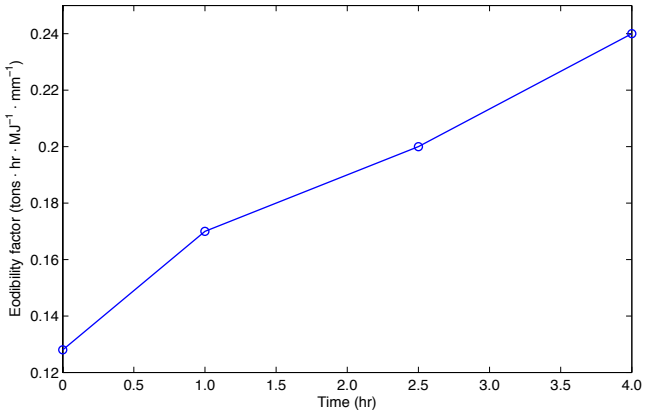

Figure 10. Empirically estimated erodibility factor of the original and fire-burned soil samples.

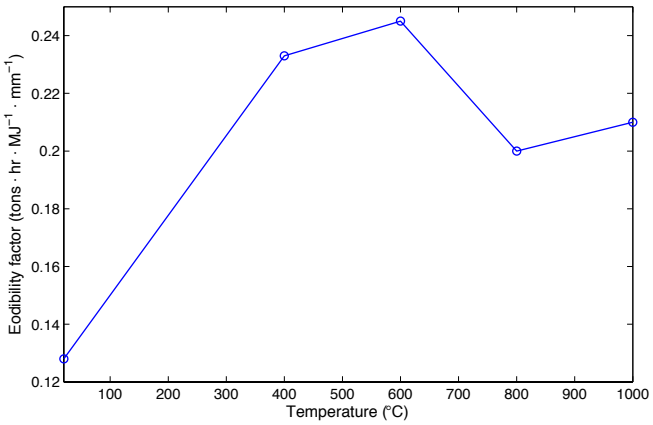

Figure 11. Empirically estimated erodibility factor of the original and oven-burned soil samples.

After the erodibility factor is estimated, the erosion rate as described in Equations (1)–(4) can be used to estimate the soil erosion rate for both fire-burned soil samples and oven-burned samples. The predicted values of the erosion rate of the fire-burned soils are plotted in Figure 12, along with the erosion rates measured in the experiments. Similarly, Figure 13 shows the results of the oven-burned samples. It is noted that the theoretical predication in Equation (1) is based on the eroded volume instead of the eroded mass; therefore, certain conversion utilizing the dry density of soil is employed to re-calibrate the experimental results of the erosion rate.

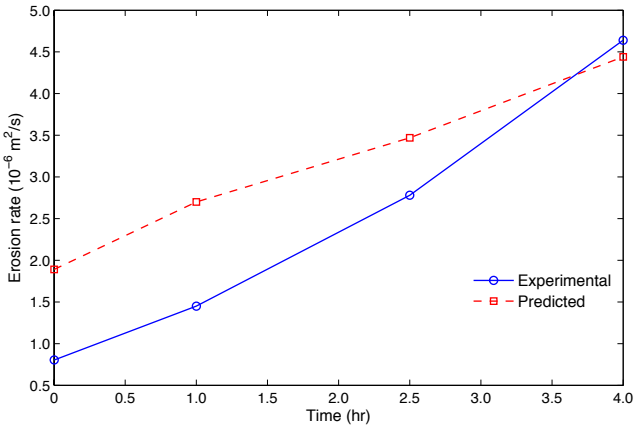

Figure 12. Experimental and empirically predicted erosion rates of the original and fire-burned soil samples.

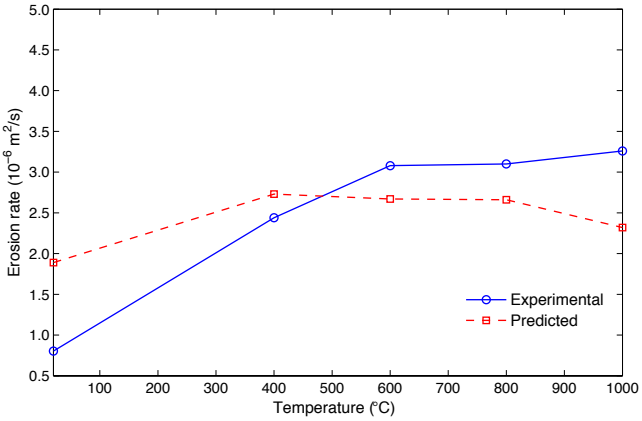

Figure 13. Experimental and empirically predicted erosion rates of the original and oven-burned soil samples.

Evidently, it is notable that the predicted erosion rate increases significantly in burned samples compared to unburned ones. In the fire-burned samples, the trend is consistent with the burning severity and, overall, the predictions grow closer to the experimental results with the burning time and severity. The results of the oven-burned samples are in the same range of order of magnitude as those of the fire-burned samples. As the burning temperature rises, overall, the erosion rate also increases, but the predicted erosion rate begins to decrease slightly at the high temperature due to the fact that the pattern of the grain size distribution is changed and the erodibility factor deceases. In this range, incidentally, the experimental erosion rates also increase very slightly, which seems to support the validity of the grain-size-based empirical predictions explored in the present study. Of course, it is worth noting that such comparisons between the experimental results and empirical predictions should be treated with caution. The empirical estimations are largely field-scale models while the laboratory specimens are generally of much smaller scale. While such inferences between the laboratory tests and numerical models are still beneficial for assessing the experimental data, further studies are much needed to examine the comprehensive characteristics of laboratory specimens and establish relevant models in their proper scale. In addition, the present study is mainly focused on the typical riverbank soil cover of clayey sand, and a comprehensive investigation of different soil types needs to be explored in future research to discover the mineral change and its effects on soil erosion. Advanced microscopic technologies such as X-ray diffraction and scanning electron microscopy may be beneficial for revealing the evolution of the

mineral composition and structure after the fire. The role of organic matter in erosion resistance needs to also be investigated for improved erosion estimation. A statistically more robust selection of sample sizes and data analysis could improve the accuracy of parameter calibration in future studies.

4. Conclusions

The present study examines some fundamental geotechnical characteristics of burned soil samples. Two burning methods are explored to simulate the effects of a wildfire on laboratory-scale soil samples. A considerable loss of organic matter was found and it increased with the rise in temperature in the oven-burned soils. The burning at 400 °C led to approximately 2% mass loss while the burning at 1000 °C led to over 10% loss. The burned soil samples lost much of their plasticity and rendered consistency limit testing impractical. Overall, the grain size distribution of burned soil samples tended to shift to a finer texture, although the results of the oven burning show that the samples burned at very high temperatures (800 °C and 1000 °C) exhibited certain nuances as they experienced a certain rebound toward the original distribution. Such subtle changes resulted in different trends in the erodibility factor and erosion rate estimated theoretically, which is based on the grain size distribution. The surface erosion was experimentally investigated and also assessed theoretically. Evidently, significantly higher erosion was found in burned soil samples than original unburned soil samples. In the fire-burned samples, the erosion rates increased consistently with higher burn severity, as the erosion rate of the lightly burned soil increased roughly 70% while it increased approximately five times more in the severely burned soil. The oven-burned samples followed a similar trend with rising temperatures, although, at the high temperatures, the increases became somewhat modest and only about three times that of the original soil. Theoretical assessment of the erosion rate and erodibility factor is explored by employing widely used empirically based prediction models. Overall, the predicted results are reasonably consistent with the experimental results. The present study demonstrates that wildfires can considerably alter soil properties that affect erosion resistance, particularly under high burning severity. Assessment of the experimental results benefits from the examination of various theoretical models where the key modeling parameters are carefully evaluated. Reliable predictions of sediment erodibility can be beneficial for geohazard risk management in identifying vulnerable areas. Improved understanding of post-fire erosion rates may assist land management agencies in the development of proper watershed rehabilitation plans. The alteration in particle size and organic matter may lead to a much broader impact that may involve plant regrowth and soil fertility during the post-fire ecosystem restoration process and should be explored in further studies. Future investigations could also consider the extension of the explored approach in the present study to field studies. How to relate the observations of the laboratory specimens to sediment responses at the field scale remains the key to better understanding the erosion processes. The roles of complex ecological factors such as vegetation covers and rainfall could also be explored in future studies of post-fire erosion.

Author Contributions: Conceptualization, L.H.; Methodology, D.S. and L.H.; Validation, D.S.; Formal analysis, D.S., J.R., K.P. and L.H.; Investigation, D.S. and J.R.; Resources, L.H.; Data curation, D.S., J.R. and K.P.; Writing—original draft, D.S. and L.H.; Visualization, K.P.; Supervision, L.H.; Project administration, L.H. All authors have read and agreed to the published version of the manuscript.

Funding: This research received no external funding.

Institutional Review Board Statement: Not applicable.

Informed Consent Statement: Not applicable.

Data Availability Statement: The original contributions presented in the study are included in the article, further inquiries can be directed to the corresponding author.

Acknowledgments: The first author (D.S.) and fourth author (L.H.) wish to acknowledge the financial support provided by the University of Toledo through a Summer Research Fellowship during the early phase of the experimental investigation in the present study.

Conflicts of Interest: The authors declare no conflicts of interest.

References

1. Waldrop, M.P.; Harden, J.W. Interactive effects of wildfire and permafrost on microbial communities and soil processes in an Alaskan black spruce forest. *Glob. Change Biol.* **2008** *14*, 2591–2602.
2. Xue, L.; Li, Q.; Chen, H. Effects of a wildfire on selected physical, chemical and biochemical soil properties in a Pinus massoniana forest in South China. *Forests* **2014** *5*, 2947–2966.
3. Santana, N.A.; Morales, C.A.S.; Silva, D.A.A.; Antoniolli, Z.I.; Jacques, R.J.S. Soil biological, chemical, and physical properties after a wildfire event in a eucalyptus forest in the pampa biome. *Rev. Bras. Cienc. Solo*, **2018**, *42*, e0170199.
4. Emelko, M.B.;Silins, U.; Bladon, K.D.; Stone, M. Implications of land disturbance on drinking water treatability in a changing climate: Demonstrating the need for “source water supply and protection" strategies. *Water Res.* **2011**, *45*, 461–472.
5. Smith, H.G.; Sheridan, G.J.; Lane, P.H.J.; Noske, P.J.; Heijnis, H. Changes to sediment sources following wildfire in a forested upland catchment, southeastern Australia. *Hydrol. Process.* **2011**, *25*, 2878–2889.
6. Pennino, M.J.; Leibowitz, S.G.; Compton, J.E.; Beyene, M.T.; LeDuc, S.D. Wildfires can increase regulated nitrate, arsenic, and disinfection byproduct violations and concentrations in public drinking water supplies. *Sci. Total Environ.* **2021**, *804*, 149890.
7. DeBano, L.F.; Neary, D.G.; Ffolliott, P.F. *Fire Effects on Ecosystems*; John Wiley & Sons: Hoboken, NJ, USA, 1998.
8. Neary, D.G. Wildfire contribution to desertification at local, regional, and global scales. In *Desertification: Past, Current and Future Trends*; Squires, V.R., Ariapour, A., Eds.; Nova Science Publishers, Inc.: Hauppauge, NY, USA, 2018; pp. 199–222.
9. O’Hara, K.C.; Ranches, J.; Roche, L.M.; Schohr, T.K.; Busch, R.C.; Maier, G.U. Impacts from wildfires on livestock health and production: Producer perspectives. *Animals* **2021**, *11*, 3230.
10. Meyer, G.A.; Wells, S.G.; Timothy Jull, A.J. Fire and alluvial chronology in Yellowstone National Park: Climatic and intrinsic controls on Holocene geomorphic processes. *Geol. Soc. Am. Bull.* **1995**, *107*, 1211–1230.
11. Cannon, S.H.; Reneau, S.L. Conditions for generation of fire-related debris flows, Capulin Canyon, New Mexico. *Earth Surf. Process. Landforms* **2000**, *25*, 1103–1121.
12. Kean, J.W.; Staley, D.M.; Lancaster, J.T.; Rengers, F.K.; Swanson, B.J.; Coe, J.A.; Hernandez, J.L.; Sigman, A.J.; Allstadt, K.E.; Lindsay, D.N. Inundation, flow dynamics, and damage in the 9 January 2018 Montecito debris-flow event, California, USA: Opportunities and challenges for post-wildfire risk assessment. *Geosphere* **2019**, *15*, 1140–1163.
13. Moody, J.A.; Kinner, D.A.; Ubeda, X. Linking hydraulic properties of fire-affected soils to infiltration and water repellency. *J. Hydrol.* **2009**, *379*, 291–303.
14. Ebel, B.A.; Moody, J.A. Rethinking infiltration in wildfire-affected soils. *Hydrol. Process.* **2013**, *27*, 1510–1514.
15. Parise, M.; Cannon, S.H. Wildfire impacts on the processes that generate debris flows in burned watersheds. *J. Hydrol.* **2012**, *61*, 217–227.
16. DeGraff, J.V.; Cannon, S.H.; Gartner, J.E. The timing of susceptibility to post-fire debris flows in the Western United States. *Environ. Eng. Geosci.* **2015**, *21*, 277–292.
17. Staley, D.M.; Negri, J.A.; Kean, J.W.; Laber, J.L.; Tillery, A.C.; Youberg, A.M. Prediction of spatially explicit rainfall intensity-duration thresholds for post-fire debris-flow generation in the western United States. *Geomorphology* **2017**, *278*, 149–162.
18. Van der Sant, R.E.; Nyman, P.; Noske, P.J.; Langhans, C.; Lane, P.N.J.; Sheridan, G.J. Quantifying relations between surface runoff and aridity after wildfire. *Earth Surf. Process. Landforms* **2018**, *43*, 2033–2044.
19. Rengers, F.K.; Tucker, G.E.; Moody, J.A.; Ebel, B.A. Illuminating wildfire erosion and deposition patterns with repeat terrestrial lidar. *J. Geophys. Res. Earth Surf.* **2016**, *121*, 588–608.
20. Orem, C.A.; Pelletier, J.D. The predominance of post-wildfire erosion in the long-term denudation of the Valles Caldera, New Mexico. *J. Geophys. Res. Earth Surf.* **2016**, *121*, 843–864.
21. Elliot, W.J.; Flanagan, D.C. Estimating WEPP cropland erodibility values from soil Properties. *J. Am. Soc. Agric. Biol. Eng.* **2023**, *66*, 329–351.
22. Benavides-Solorio, J.D.D.; MacDonald, L.H. Measurement and prediction of post-fire erosion at the hillslope scale, Colorado Front Range. *Int. J. Wildland Fire* **2005**, *14*, 457–474.
23. Turnbull, L.; Wainwright, J.; Brazier, R.F. Changes in hydrology and erosion over a transition from grassland to shrubland. *Hydrol. Process.* **2010**, *24*, 393–414.

24. McGuire, L.A.; Kean, J.W.; Staley, D.M.; Rengers, F.K.; Wasklewicz, T.A. Constraining the relative importance of raindrop- and flow-driven sediment transport mechanisms in postwildfire environments and implications for recovery time scales. *J. Geophys. Res. Earth Surf.* **2016**, *121*, 2211–2237.
25. Havel, A.; Tasdighi1, A.; Arabi1, M. Assessing the hydrologic response to wildfires in mountainous regions. *Hydrol. Earth Syst. Sci.* **2018**, *22*, 2527–2550.
26. Hallema, D.W.; Sun, G.; Bladon, K.D.; Norman, S.P.; Caldwell, P.V.; Liu, Y.; McNulty, S.G. Regional patterns of postwildfire streamflow response in the Western United States: The importance of scale-specific connectivity. *Hydrol. Process.* **2017**, *31*, 2582–2598.
27. Garcia-Corona, R.; Benito, E.; de Blas, E.; Varela, M.E. Effects of heating on some soil physical properties related to its hydrological behaviour in two north-western Spanish soils. *Int. J. Wildland Fire* **2004**, *13*, 195–199.
28. McGuire, L.A.; Youberg, A.M. Impacts of successive wildfire on soil hydraulic properties: Implications for debris flow hazards and system resilience. *Earth Surf. Process. Landforms* **2019**, *44*, 2236–2250.
29. Cerda, A.; Imeson, A.C.; Calvo, A. Fire and aspect induced differences on the erodibility and hydrology of soils at La Costera, Valencia, southeast Spain. *Catena* **1995**, *24*, 289–304.
30. Follmi, D.; Baartman, J.E.M.; Benali, A.; Nunes, J.P. How do large wildfires impact sediment redistribution over multiple decades? *Earth Surf. Process. Landforms* **2022** *47*, 3033–3050.
31. Yang, X.; Zhang, M.; Oliveira, L.; Ollivier, Q.R.; Faulkner, S.; Roff, A. Rapid assessment of hillslope erosion risk after the 2019–2020 wildfires and storm events in Sydney Drinking Water Catchment. *Remote Sens.* **2020**, *12*, 3805.
32. Noske, P.J.; Nyman, P.; Lane, P.N.J.; Rengers, F.K.; Sheridan, G.J. Changes in soil erosion caused by wildfire: A conceptual biogeographic model. *Geomorphology* **2024**, *459*, 109272.
33. Ebel, B.A.; Romero, O.C.; Martin, D.A. Thresholds and relations for soil-hydraulic and soil-physical properties as a function of burn severity 4 years after the 2011 Las Conchas Fire, New Mexico, USA. *Hydrol. Process.* **2018**, *32*, 2263–2278.
34. Ahaneku, I.E.; Ezinna, K.C.; Orji, F.N.; Alaneme, G.U.; Chukwudi, E.M. Spatial distribution of soil erodibility factors in erosion-prone areas in Umuahia, Southeast, Nigeria. *J. Eng. Res.* **2024**, *in press*. https://doi.org/10.1016/j.jer.2024.04.002.
35. Wells, C.G.; Campbell, R.E.; DeBano, L.F.; Lewis, C.E.; Fredriksen, R.L.; Franklin, E.C.; Froelich, R.C.; Dunn, P.H. 1979. *Effects of Fire on Soil: A State of Knowledge Review*; U.S. Department of Agriculture, Forest Service: Washington, DC, USA, 1979.
36. Floyd, A. Effect of fire upon weed seeds in the wet sclerophyll forests of northern New South Wales. *Aust. J. Bot.* **1966**, *14*, 243–256.
37. DeBano, L.F.; Rice, R.M.; Eugene, C.C. *Soil Heating in Chaparral Fires: Effects on Soil Properties, Plant Nutrients, Erosion, and Runoff*; Research Paper PSW-RP-145; US Department of Agriculture, Forest Service, Pacific Southwest Forest and Range Experiment Station: Berkeley, CA, USA, 1979.
38. Biederbeck, V.; Campbell, C.; Bowren, K.; Schnitzer, M.; McIver, R. Effect of burning cereal straw on soil properties and grain yields in Saskatchewan. *Soil Sci. Soc. Am. J.* **1980**, *44*, 103–111.
39. Hubbert, K.R.; Preisler, H.K.; Wohlgemuth, P.M.; Graham, R.C.; Narog, M.G. Prescribed burning effects on soil physical properties and soil water repellency in a steep chaparral watershed, southern California, USA. *Geoderma* **2006**, *130*, 284–298.
40. Granged, A.J.; Zavala, L.M.; Jordan, A.; Barcenas-Moreno, G. Post-fire evolution of soil properties and vegetation cover in a Mediterranean heathland after experimental burning: A 3-year study. *Geoderma* **2011**, *164*, 85–94.
41. Chief, K.; Young, M.H.; Shafer, D.S. Changes in soil structure and hydraulic properties in a wooded-shrubland ecosystem following a prescribed fire. *Soil Sci. Soc. Am. J.* **2012**, *76*, 1965–1977.
42. Giovannini, G.; Lucchesi, S.; Giachetti, M. Effect of heating on some physical and chemical parameters related to soil aggregation and erodibility. *Soil Sci.* **1988**, *146*, 255–262.
43. Ulery, A.L.; Graham, R.C. Forest fire effects on soil color and texture. *Soil Sci. Soc. Am. J.* **1993**, *57*, 135–140.
44. Wischmeier, W.H.; Smith, D.D. *Predicting Rainfall Erosion Losses—A Guide to Conservation Planning*; The USDA Handbook No. 537; Department of Agriculture, Agricultural Research Service: Washington, DC, USA, 1978.
45. Renard, K.; Foster, G.; Weesies, G.; McCool, D.; Yoder, D. *Predicting Soil Erosion by Water: A Guide to Conservation Planning With the Revised Universal Soil Loss Equation (RUSLE)*; The USDA Handbook No. 703; Department of Agriculture, Agricultural Research Service: Washington, DC, USA, 1997.
46. Wang, H.; Zhao, H. Dynamic changes of soil erosion in the Tahoe River basin using the RUSLE model and google earth engine. *Water* **2020**, *12*, 1293.
47. Melese, T.; Senamaw, A.; Belay, T.; Bayable, G. The spatiotemporal dynamics of land use land cover change, and its impact on soil erosion in Tagawa watershed, Blue Nile basin. *Ethiopia. Glob. Chall.* **2021**, *5*, 2000109.
48. Foster, G.R.; Toy, T.E.; Renard, K.G. Comparison of the USLE, RUSLE1.06c, and RUSLE2 for Application to Highly Disturbed Lands. In *First Interagency Conference on Research in Watersheds*; U.S. Department of Agriculture: Washington, DC, USA, 2003; pp. 154–160.
49. David, W.P. Soil and Water Conservation Planning: Policy Issues and Recommendations. *J. Philipp. Dev.* **1988**, *15*, 47–84.

50. Fernandez, C.; Wu, J.; McCool, D.; Stoeckle, C. Estimating water erosion and sediment yield with GIS, RUSLE, and SEDD. *J. Soil Water Conserv.* **2003**, *58*, 128–136.
51. Chen, L.; Qian, X.; Shi, Y. Critical area identification of potential soil loss in a typical watershed of the three Gorges reservoir region. *Water Resour. Manag.* **2011**, *25*, 3445–3463.
52. Panagos, P.; Borrelli, P.; Poesen, J.; Ballabio, C.; Lugato, E.; Meusburger, K.; Alewell, C. The new assessment of soil 20 loss by water erosion in Europe. *Environ. Sci. Policy* **2015**, *54*, 438–447.
53. Fernandez, M.A.; Daigneault, A. Erosion mitigation in the Waikato District, New Zealand: Economic implications for agriculture. *Int. J. Food Agric. Econ.* **2016**, *48*, 341–361.
54. Smith, R.E.; Goodrich, D.C.; Woolhiser, D.A.; Unkrich, C.L. KINEROS—A kinematic runoff and erosion model. In *Computer Models of Watershed Hydrology*; Singh, V.P., Ed.; Water Resources Publications: Fort Collins, CO, USA, 1995; pp. 697–732.
55. Laflen, J.M.; Lane, L.J.; Foster, G.R. WEPP: A new generation of erosion prediction technology. *J. Soil Water Conserv.* **1991**, *46*, 34–38.
56. Goodrich, D.C.; Unkrich, C.L.; Smith, R.E.; Woolhiser, D.A. KINEROS2—A distributed kinematic runoff and erosion model. In Proceedings of the 2nd Federal Interagency Hydrologic Modeling Conference, Las Vegas, NV, USA, 28 July–1 August 2002; pp. 1–14.
57. Gassman, P.W.; Reyes, M.R.; Green, C.H.; Arnold, J.G. The Soil and Water Assessment Tool: Historical development, applications, and future research directions *Trans. ASABE* **2007**, *50*, 1211–1250.
58. Sidman, G.; Guertin, D.P.; Goodrich, D.C.; Unkrich, C.L.; Burns, I.S. Risk assessment of post-wildfire hydrological response in semiarid basins: The effects of varying rainfall representations in the KINEROS2/AGWA model. *Int. J. Wildland Fire* **2015**, *25*, 268–278.
59. Hajigholizadeh, M.; Melesse, A.M.; Fuentes, H.R. Erosion and sediment transport modelling in shallow waters: A review on approaches, models and applications. *Int. J. Environ. Res. Public Health* **2018**, *15*, 518.
60. HKorgaonkar, Y.; Guertin, D.P;, Goodrich, D.C.; Unkrich, C.; Kepner, W.G.; Burns, I.S. Modeling urban hydrology and green infrastructure using the AGWA urban tool and the KINEROS2 model. *Front. Built Environ.* **2018**, *4*, 58.
61. Vanini, H.S.; Amini, M. Assessment of soil erosion on hillslopes (A case study carried out in the Ashan Drainage Basin, Iran). *Eur. J. Environ. Sci.* **2017**, *7*, 99–107.
62. Feng, N.; Liu, D.; She, D. Effects of vegetation restoration on carbonate-derived laterite erodibility in karst mountain areas. *Land Degrad. Dev.* **2021**, *33*, 1347–1365.
63. Zhu, G.; Tang, Z.; Shangguan, Z.; Peng, C.; Deng, L. Factors affecting thes spatial and temporal variations in soil erodibility of China. *J. Geophys. Res. Earth Surf.* **2019**, *124*, 737–749.
64. El-Swaify, S.A.; Dangler, E.W. Erodibilities of selected tropical soils in relation to structural and hydrologic parameters. In Proceedings of the National Conference on Soil Erosion, West Lafayette, IN, USA, 24–26 May 1976; pp. 105–114.
65. Williams, J.R.; Renard, K.G.; Dyke, P.T. EPIC: A new method for assessing erosion's effect on soil productivity. *J. Soil Water Conserv.* **1983** *38*, 381–383.
66. Merzouk, A. Relative Erodibility of Nine Selected Moroccan Soils as Related to Their Physical, Chemical and Mineralogical Properties. PhD Thesis, University of Minesota, St. Paul, MN, USA, 1985.
67. Engelund, F.; Hansen, E. *A Monograph on Sediment Transport in Alluvial Streams*; Technical University of Denmark: Copenhagen, Denmark, 1967.
68. Julien, P.Y.; Simons D.B. Sediment transport capacity of overland flow. *Trans. ASAE* **1985**, *28*, 755–762.
69. Semmens, D.J.; Goodrich, D.C.; Unkrich, C.L.; Smith, R.E.; Woolhiser, D.A.; Miller, S.N.; Wheater, H.; Sorooshian, S.; Sharma, K.D. KINEROS2 and the AGWA modelling framework. In *Hydrological Modelling in Arid and Semi-Arid Areas*; Cambridge University Press: Cambridge, UK, 2007; pp. 49–68.